Angular dependence of rotational and vibrational energies of product CO_2 in CO oxidation on Pd(110)

Toshiro Yamanaka[*a]

[a]*Catalysis Research Center, Hokkaido University, Sapporo 001-0021, Japan. E-mail: yama@cat.hokudai.ac.jp*

Rotational and vibrational energies of product CO_2 in CO oxidation on Pd(110) surfaces were measured as functions of desorption angles. The antisymmetric vibrational temperature (T_a) was separately determined from the other vibrational modes from the normalized chemiluminescence intensity. The rotational temperature (T_{rot}) and vibrational temperature averaged over the symmetric and bending modes (T_{sb}) were then determined by the position and width of spectra by comparison with simulated spectra. On Pd(110)-(1×1), with increases in desorption angle, T_a, T_{sb} and T_{rot} decreased in the [001] direction but remained constant in [1$\bar{1}$0]. However, such anisotropy disappeared when the ratio of exposure of O_2 to that of CO decreased, resulting in a gradual decrease of the three temperatures with increases in the desorption angle. On Pd(110) with missing-rows, the three temperatures increased in [001] but decreased in [1$\bar{1}$0], indicating that the transition state changes with the geometry of the substrate. On Pd(110) with missing-rows, T_a was significantly lower than T_{sb}, although T_a was close to or higher than T_{sb} on Pd(110)-(1×1). However, there was no significant difference in angular dependence between T_a, T_{sb} and T_{rot}.

1. Introduction

It is important to elucidate energy transfer dynamics and structures of transition states (TSs) for a full understanding of surface reaction.[1-6] The dynamics and TS structures strongly depend on microscopic structures of substrates. Such an understanding at the atomic level is required to develop superior catalysts, electrodes, and material growth processes.

Dynamics and TS structures have been studied by measurements of translational and internal (rotational and vibrational) energies of desorbing products in surface scattering and reaction processes.[2-17] However, angle-resolved (AR) measurements[6-12] of internal energies have long been lacking in thermal surface reactions because of the difficulty in conducting such experiments,[18] although such measurements are required in order to obtain detailed structural information. In this paper, results of measurements of internal energies of AR product CO_2 in CO oxidation on Pd(110) are presented.

CO oxidation on noble metals is one of the most extensively studied prototypical surface reactions. Because of its practical importance and various phenomena, this reaction has long attracted attention of chemists and physicists.[1,6,13-22] This reaction proceeds through (i) adsorption of CO and dissociative adsorption of O_2, (ii) diffusion of CO towards an O adatom to form a TS (O-CO-metal complex), and then (iii) repulsive desorption of CO_2. Details of structures and energies during formation processes of the TS have been studied by ab initio calculations.[19-21] During desorption of CO_2, the excess energy is distributed into translational, vibrational and rotational modes of CO_2, although some parts of the excess energy flow into substrates. Since nascent CO_2 receives strong repulsion from the surface, desorption of CO_2 is sharply collimated in the direction normal to the CO_2 formation site. The translational temperature of CO_2 (T_{trans}) is much higher than the surface temperature of the sample (T_{sample}). In addition, T_{trans} shows a maximum at the collimation angle.[6] Thus, angular dependence of flux and T_{trans} of desorbing CO_2 involves structures of TS and substrate. It is expected that energy partition into internal modes also changes with changes in desorption angle.

Non-AR measurements of internal energies of product CO_2 have been extensively conducted by analysis of chemiluminescence from CO_2[13-15,17] and infrared absorption by CO_2.[16] However, until recently the angular dependence of T_{rot} and T_{vib} has not been studied because the intensity of chemiluminescence is lowered by three orders in AR measurements.[18] Such measurements of internal energies of AR-CO_2 have recently been reported.[18,23] However, information obtained from these measurements is still limited. That is, while CO_2 has three vibrational modes (symmetric stretch (S), bending (B), and antisymmetric stretch (A) modes), in the above AR study only rotational temperature (T_{rot}) and vibrational temperature (T_{vib}) averaged over the three modes were determined assuming $T_{vib} = T_s = T_b = T_a$ (temperatures of S, B, and A modes).

In this paper, results of mode-resolved AR measurements of vibrational energies of product CO_2 on Pd(110) are presented. The intensity of chemiluminescence from AR product CO_2 was analyzed in comparison with that from high-temperature reference CO_2 from a molecular beam source, and T_a was separately determined. The temperature averaged over the symmetric stretch and bending modes (T_{sb}) was also estimated as functions of the desorption angles.

2. Experimental

The difficulty in measurements of internal energies of AR-CO_2 and design of an apparatus for analysis of extremely weak infrared emission from AR-CO_2 have recently been described in detail.[18] Infrared chemiluminescence during relaxation of the antisymmetric stretch mode of CO_2 after passing through two slits for angle selection, $(n_s, n_b, n_a) \rightarrow (n_s, n_b, n_a\text{-}1)$, where n_s, n_b and n_a are the quantum numbers of S, B and A modes, respectively, was analyzed by an FT-IR spectrometer. The apparatus consists of three parts separated by two slits, and each of the three parts was evacuated independently. The azimuthal direction of a clean Pd(110) surface was determined by LEED observation by using another ultra-high-vacuum apparatus, although LEED patterns of Pd(110) surfaces adsorbed by oxygen or CO were not observed. In the reaction chamber of the present apparatus, the Pd(111) surface of 10 mm in diameter was cleaned by Ar sputtering and

heating in an oxygen atmosphere. Then the surface was set in front of the first slit. O_2 and CO were sprayed from four dosers on the surface kept at desired temperatures (T_{sample}) for CO oxidation to proceed. The desorption angle was changed by rotating the sample and dosers together.

In the present study, first T_a was determined by careful analysis of chemiluminescence intensity and then T_{sb} and T_{rot} were determined by curve fitting. To compare the intensity from AR product CO_2 with that from reference high-temperature CO_2, a diffusive molecular beam source was newly developed. Either a Pd(111) surface or diffusive beam source (1400 K) of reference CO_2 was set before the first slit, and chemiluminescence from product CO_2 and reference CO_2 was detected, as shown in Fig. 1a. Before analysis of chemiluminescence intensities, the intensities were normalized by the amount of CO_2 measured by a quadrapole mass spectrometer placed after the second slit.

An outline of the beam source is shown in Fig. 1b. After the CO_2 beam passed through two slits, the chemiluminescence from the CO_2 beam was detected in the same way as that for product CO_2. CO_2 was introduced into a Mo tube kept at 1400 K. The temperature of the Mo tube was monitored with a thermo-couple attached at the middle point of the tube. The tube was covered by Ta double shields and copper double shields cooled by water. CO_2 introduced into the tube was emitted from a capillary hole of 0.5 mm in diameter and 4 mm in length. Then the CO_2 beam was laterally directed by the final nozzle, which is a Mo plate of 1 mm in thickness and 10 mm in diameter with seven holes that are each 1 mm in diameter. It was calculated that each hole of which the length and diameter are equal yields an angular distribution of CO_2 close to a $\cos^6\theta$ form.[24] This distribution is close to that of product CO_2 in CO oxidation on a Pd single crystal of 10 mm in diameter. Thus, the CO_2 from the beam source penetrates two slits in a similar way to that of product CO_2 in CO oxidation on Pd(110) surfaces of 10 mm in diameter, and all conditions of chemiluminescence measurements are invariant for product CO_2 and reference CO_2. The position of the beam source was optimized by checking images of the beam source reflected by two mirrors under the beam source (view 1) and in the emission collector chamber (view 2).

Fig. 1c shows a chemiluminescence spectrum from reference CO_2. The resolution of wavenumbers was 4 cm^{-1}. At this resolution, chemiluminescence spectra show a single broad peak from 2400 to 2200 cm^{-1} as shown in Fig. 1c. This peak consists of a large number of transition lines from various rovibrational states. In previous works the populations of rotational and vibrational states were expressed by rotational and vibrational temperatures.[13-18,23,25-27] These expressions using temperatures may not be valid because previous works were conducted at high reactant pressures and population of rovibrational states of CO_2 after being scattered with reactants were studied. In order to obtain accurate populations of rovibrational states, state-resolved measurements should be conducted at low reactant pressures. Although the effect of collision was sufficiently suppressed in the present measurements, state-resolved measurements are not possible due to extremely weak chemiluminescence signals. Therefore, in the present study, the rovibrational population was expressed by using temperatures as in previous works.

First, T_{vib} and T_{rot} were determined by a curve fitting procedure.[13,17,23,25] The spectrum is wide when T_{rot} is high, while the spectrum is more red-shifted when T_s, T_b and T_a are high. In the simulation, the ratio of redshift with increases in T_s, T_b, and T_a was about 1:2:1.3. It is not possible to separately determine T_s, T_b, and T_a only from the degree of redshift, and therefore T_{vib} averaged over the three modes (i.e., assuming $T_{vib}=T_a= T_s= T_b$) and T_{rot} were determined.[13,17,25] The thick curve in Fig. 3c shows the best simulated result yielding T_{vib} =1200 K and T_{rot}=1150 K. These values are lower than 1400 K probably because the temperature around the final nozzle is lower than the middle point of the Mo tube. Since the two values are close, the internal modes are almost in equilibrium, i.e., $T_a \approx$ 1200 K. The total chemiluminescence intensity changes with T_a in the following form as shown by the solid curve in Fig. 1d:

$$I_{total} = \sum_{na=1}^{\infty} {R_V}^2 \exp(-E_{na} / kT_a) / \sum_{na=0}^{\infty} \exp(-E_{na} / kT_a) \qquad (1),$$

where ${R_v}^2$ is Frank-Condon factors, and E_{na} is the energy of antisymmetric vibration. In Fig. 1d, the theoretical curve is normalized so that I_{total} at T_a=1200 K (T_a of reference CO_2) becomes

unity. T_a of product CO_2 can be determined by comparison of chemiluminescence intensities normalized by CO_2 amount between product CO_2 and reference CO_2, by plotting total intensities normalized to CO_2 mass signals on the curve in Fig. 1c. For example, T_a of product CO_2 at O_2/CO=1/2 (O_2/CO being the ratio of exposure of O_2 to that of CO) and θ=0º is determined to be 1400 K, and T_a decreased to 1050 K at θ=40º. After T_a is determined, T_{sb} and T_{rot} of product CO_2 can be determined by curve fitting.[13,18,23, 25-27] The spectra are more red-shifted when T_{sb} is higher, and the width of spectra is larger when T_{rot} is higher. T_s and T_b cannot be separately obtained only from the degree of redshift and therefore T_{sb}=T_s=T_b was assumed in the simulation. The contribution of the B mode to T_{sb} is twice that of the S mode since CO_2 has two kinds of B modes of which vibrational directions are perpendicular to each other. Figure 2 shows typical chemiluminescence spectra from product CO_2 at two different desorption angles at O_2/CO=1/2 and the total exposure of 4.5×10^{17} molecules/cm^{2}s. The values of T_a, T_{sb}, and T_{rot} were 1400 K, 1530 K and 950 K (0˚), and 1050 K, 1250 K and 550 K (40˚ in [001]), respectively.

In previous works, T_a of product CO_2 in CO oxidation on Pd surfaces was estimated by chemiluminescence intensity.[25-27] The basic idea is the same as the present method, but there are some different points. That is, in the previous works (i) the intensity is assumed to be proportional to $\exp(-E_{na}/kT_a)$, and (ii) T_{sb} was estimated from values of T_{vib} and T_a by using a formula, $T_{vib} = (T_a + 3T_{sb})/4$.

3. Results

3.1 CO_2 formation rate

Figure 3 shows the rate of CO_2 formation as a function of T_{sample} for various O_2/CO ratios at a fixed total exposure of 4.5×10^{17} molecules/cm^{2}s. At each ratio, with increasing T_{sample}, the CO_2 formation becomes noticeable above 500 K and shows a maximum at around 550-750 K (T_{max}). Below T_{max}, the oxygen dissociation is rate-determining in the CO oxidation, and the surface is highly covered by CO, that is, CO(a)>>O(a). The O_2 dissociation increases at higher T_{sample} by

increasing vacant sites through enhanced CO desorption. On the other hand, above T_{max}, the coverage of CO is reduced, resulting in a decrease in CO_2 formation. T_{max} shifted to higher values as the O_2/CO ratio decreased because of the higher temperature required to yield vacant sites at high CO pressures.[1,6,25] AR measurements were performed at T_{sample} = 600 K and O_2/CO = 2, 1/2, and 1/8 as shown below.

3.2 Angular dependence of T_a, T_{sb} and T_{rot}

Figures 4a shows angular dependence of T_a, T_{sb} and T_{rot} in [1$\bar{1}$0] and [001] directions at O_2/CO = 2. T_a, T_{sb} and T_{rot} at 0º are 1000 K, 1450 K and 800 K, respectively. All of these temperatures decreased with increases in the desorption angle in [1 $\bar{1}$ 0]. In contrast, these temperatures increased in [001].

When O_2/CO decreased to 1/2, T_a significantly increased to 1400 K at 0º. T_{rot} also increased to 950 K at 0º, as shown in Fig. 4b. At this O_2/CO ratio, the anisotropy was reversed. That is, all temperatures remained constant when the desorption angle changed in [1$\bar{1}$0], while these temperatures decreased in [001].

When O_2/CO further decreased to 1/8, T_a further increased and became higher than T_{sb}. At this O_2/CO ratio, the anisotropy almost disappeared. That is, T_a was almost constant in both azimuthal directions, and T_{sb} and T_{rot} decreased in both azimuthal directions, as shown in Fig. 4c.

4. Discussion

4.1 Angular dependence of T_a, T_{sb} and T_{rot}, and TS structures

In the present study, in situ LEED observations of Pd(110) surfaces under CO oxidation to elucidate surface structures were not been conducted because LEED observation under reactant pressures as high as 10^{-3} Torr is difficult. However, it is known that the (1×1) structure of clean Pd(110) (Fig. 5a) is reconstructed into a missing-row structure (i.e., c(2×4)-O (Fig. 5b)) above 360

K when the oxygen coverage is high.[28,29] Therefore, the surface structures of Pd(110) at T_{sample} = 600 K are assumed to be (1×1) and missing-row structures at O_2/CO≤1/2 and at O_2/CO=2, respectively. The above results show clear dependence of T_a, T_{sb} and T_{rot} of product CO_2 on polar and azimuth angles. Since results for Pd(110) at O_2/CO = 1/2 and at O_2/CO = 2 are quite different, the observed angular dependence of T_a, T_{sb} and T_{rot} contains information on structures of surfaces and TS structures on them.

At O_2/CO = 1/2 (Pd(110)-(1×1)), T_a, T_{sb} and T_{rot} in the y-z plane (see the illustration in Fig. 5a) were all almost constant, while these temperatures decreased with increases in θ in the x-z plane, as shown in Fig. 4b. This suggests that CO_2 with high rovibrational energy can easily move in the y-z plane but that its motion in the x-z plane is hindered. It was proposed that CO approaches an oxygen atom at the bottom of the atomic trough to react on this surface.[6,30] The present results suggest that the TS is oriented in the y-z plane and that it receives repulsion along the z-axis, resulting in rotational motion in the y-z plane. In this case, nascent CO_2 can easily move in the y-z plane, but its motion in the x-z plane is hindered by rows of the 1st Pd layers. As θ increases, the translational temperature and desorption flux of CO_2 gradually decrease in the y-z plane and decrease rapidly in the x-z plane,[6,30] consistent with restricted motions of CO_2 within the y-z plane.

At O_2/CO = 1/8, the surface is covered by CO. The anisotropy of T_{sb}, T_a and T_{rot} disappeared, and all temperatures decreased with increases in desorption angle in both azimuthal directions. This is probably because the energy of CO_2 is lost through scattering with neighboring adsorbed CO when CO_2 is desorbed in inclined directions. The decrease of T_a at high desorption angles is less significant, suggesting that the energy relaxation of the antisymmetric mode through scattering between nascent CO_2 and CO is a slow process.

On Pd(110) with missing-rows, T_a, T_{sb} and T_{rot} increased with increases in θ in the x-z plane and decreased in the y-z plane. These results indicate that desorption of CO_2 with high rovibrational energy is promoted at large θ in the x-z plane. Since oxygen atoms form zigzag chains along the y-axis near protruding rows of the 1st Pd layer (Fig. 5b)[29] and the oxygen at the end of the

chain shows high reactivity with CO,[31] CO oxidation is thought to occur near the protruded rows. In this case, the TS can be oriented in the x-z plane and rotational motion in the x-z plane is easy as shown in Fig. 5b. Depending on the position and inclination of the TS, the direction of repulsion from protruding rows may shift from the surface normal in the x-z plane, and also the torque operative to the TS may change. Thus, desorption of CO_2 with high rotational energy at large θ in the x-z plane is promoted. A TS oriented in the plane perpendicular to the atomic rows was predicted by ab initio calculations for CO oxidation on Pt(110) with missing-rows, which is similar to the present Pd(110) with missing-rows,[32] consistent with the prediction in the present work.

More detailed pictures are considered as follows. In CO oxidation, CO approaches O to form a TS since diffusion of CO is much faster than that of O.[6] The TS has Pd-O, Pd-C, and new O-C bonds.[19-21] When CO_2 forms, it receives strong repulsion from the substrate. This is Pauli repulsion,[6] which is operative between electrons of CO_2 and those of the Pd substrate when Pd-O and Pd-C bonds become antibonding. In many desorption processes, the product receives repulsion along the direction of the bond that breaks. In many CO_2 formation processes, CO_2 is desorbed in the direction normal to the CO_2 formation site.[6] The sum of repulsions along Pd-O and Pd-C bonds may result in a repulsion of which the direction is close to normal to the formation site, although the direction of each bond may not be normal to the formation site.

In the TS, bonds of Pd-O, Pd-CO, and O-CO compete with each other.[19-21] When the Pd-O bond is strong and the Pd-CO bond is weak (TS(α) in Fig. 5c), the distance between O and Pd is short, while that between C and Pd is long. Nascent CO_2 receives repulsion mainly at the O end far from the center-of-mass at the moment of breaking of the Pd-O bond. Since nascent CO_2 appears on the inclined (111) facet, the direction of repulsion is inclined toward the (111) facet normal. This results in desorption of CO_2 with high T_{rot} in inclined directions.

In another case, CO may bond with Pd atoms in the 1st layer to form a TS and O may be somewhat repelled by CO (TS(β) in Fig. 5d) since ab initio calculations of CO oxidation often show that the competition between CO and O to bind the same Pd atom leads to breaking of the O-Pd

bond and repelling of O by CO to an adjacent site.[19-21] Nascent CO_2 receives repulsion mainly at the C end close to the center-of-mass, resulting in desorption of CO_2 with low T_{rot}. Since CO_2 appears near a protruding row of Pd atoms, this CO_2 receives repulsion in the direction close to the surface normal direction. Thus, T_{rot} is low at the surface normal direction. Also, a TS that is similar to TS(β) may be formed near the protruding row of Pd atoms when CO approaches O at the opposite side of the zigzag chain (TS(γ) in Fig. 5e). This TS would also result in desorption of CO_2 with low T_{rot} at the surface normal direction. In these cases, the geometry of TS can be more linear and closer to that of gas-phase CO_2 since the substrate structure at the protruded atomic row is widely opened. In this case, the bending and shrinking/stretching of TS or nascent CO_2 forced by the substrate structure should be less, resulting in lower T_a and T_{sb} at the surface normal direction.

For the TS geometries proposed above, motions of symmetric stretch, bending, and antisymmetric stretch modes are in the y-z plane on Pd(110)(1×1) and in the x-z plane on Pd(110) with missing-rows. The present results indicate that desorption of CO_2 with high vibrational energy is concentrated in the y-z plane on Pd(110)(1×1) (Fig. 4b) and in the x-z plane on Pd(110) with missing-rows (Fig. 4a). During the desorption process, the bent TS[19-21] becomes linear and the C-O bond lengths approach that of gas-phase CO_2, resulting in vibrational excitation, during which translational excitation also occurs. These structural changes from TS to linear CO_2 may also induce an impulse accelerating the translational motion in the same plane as that of vibration. Since motions of antisymmetric mode and bending mode are perpendicular to each other in a single CO_2 molecule, it is expected that T_a and T_{sb} are enhanced at different desorption angles. Nevertheless, such a difference was not observed in the present study. This is probably because TS is oriented at various angles in the y-z plane on Pd(110)(1×1) and in the x-z plane on Pd(110) with missing-rows.

4.2 Coverage dependence of each temperature

In the present study, chemiluminescence intensity normalized by CO_2 mass signals increased by about 4 times when O_2/CO decreased from 2 to 1/8. By plotting the normalized intensities in Fig.

1c, it was found that T_a is strongly dependent on O_2/CO. At O_2/CO = 2, T_a is about 1000 K and it increased to about 1400 K at O_2/CO = 1/2. At O_2/CO = 1/8 T_a is about 1600 K and this value exceeds that of T_{sb} (about 1400 K). On the other hand, T_{sb} is always 1400 to 1500 K and less dependent on the O_2/CO ratio, although it gradually decreased with decreases in O_2/CO. Such increment of T_a and decrease in T_{sb} were previously reported by Kunimori's group.[25] Their results showed that chemiluminescence intensity normalized by CO_2 mass signals at O_2/CO = 1/8 is about 4-times higher than that at O_2/CO = 2, which is consistent with the present results. The general trends of their results and the present results are similar, but the values of T_a in the present study are lower than their results (T_a=1500 K (O_2/CO=2) and 2800 K (O_2/CO=1/8)). The inconsistency in T_a values between the previous and present results may be partly because the formula used to estimate T_a (eq. (1)) is different from that used in the previous study.[25]

In the present study, the increment of T_a was significant when O_2/CO decreased from 2 to 1/2 but less significant when O_2/CO decreased from 1/2 to 1/8. The anisotropy in angular dependence of T_a, T_{sb} and T_{rot} was reversed when O_2/CO decreased from 2 to 1/2, and surface reconstruction is thought to have occurred from missing-row to 1×1 structures, resulting in change in orientation of TSs from the x-z plane to y-z plane. This suggests that increase in T_a is related to this change in TS structure. In the previous work,[25] it was proposed that increased T_a is due to the TS structure in which the distance between O and CO is compressed due to increased CO coverage. This mechanism does not seem to be inconsistent with the present results.

V. Conclusions

Rotational and vibrational energies of product CO_2 in CO oxidation on Pd(110) surfaces were studied as functions of polar and azimuth angles at three O_2/CO ratios, 2, 1/2 and 1/8. The surface is thought to be a (1×1) structure at O_2/CO = 1/2 and 1/8 and to be a missing-row structure at O_2/CO = 2. The antisymmetric vibrational temperature (T_a) was separately determined from the

vibrational temperature averaged over the symmetric and bending modes (T_{sb}) from the normalized chemiluminescence intensity. The results are summarized as follows.

(i) On Pd(110)-(1×1) at O_2/CO = 1/2, T_{rot}, T_a and T_{sb} decreased in the [001] direction but remained constant in [1$\bar{1}$0] with increases in desorption angle.

(ii) The above anisotropy disappeared when O_2/CO decreased to 1/8, resulting in gradual decrease of T_{rot}, T_a and T_{sb} with increases in desorption angle in both azimuthal directions.

(iii) On Pd(110) with missing-rows at O_2/CO = 2, all temperatures increased in [001] but decreased in [1$\bar{1}$0], indicating that the transition state changes with geometry of the substrate.

(iv) On Pd(110) with missing-rows, T_a was significantly lower than T_{sb}, although T_a increased to exceed T_{sb} when O_2/CO decreased and the surface structure became a (1×1) structure.

(V) There was no significant difference in angular dependence between T_{rot}, T_a and T_{sb}.

References

[1] R. Imbihl and G. Ertl, *Chem. Rev.*, 1995, **95**, 697-733.

[2] F. M. Zimmermann and W. Ho, *Surf. Sci. Rep.*, 1995, **22**, 127-247.

[3] A. Hodgson, Prog. *Surf. Sci.*, 2000, **63**, 1-61.

[4] H. A. Michelsen, C. T. Rettner and D. J. Auerbach, *Phys. Rev. Lett.*, 1992, **69**, 2678-2681.

[5] C. T. Rettner and D. J. Auerbach, *Phys. Rev. Lett.*, 1995, **74**, 4551-4554.

[6] T. Matsushima, *Surf. Sci. Rep.*, 2003, **52**, 1-62.

[7] R. T. Jongma, G. Berden, T. Rasing, H. Zacharias and G. Meijer, *J. Chem. Phys.*, 1997, **107**, 252-261.

[8] H. Vach, A. De Martino, M. Benslimane, M. Chatelet and F. Pradere, *J. Chem. Phys.*, 1994, **100**, 8526-8536.

[9] F. H. Geuzebroek, A. E. Wiskerke, M. G. Tenner, A. W. Kleyn, S. Stolte and A. Namiki, *J. Phys. Chem.*, 1991, **95**, 8409-8421.

[10] C. T. Rettner and D. J. Auerbach, *Science*, 1994, **263**, 365-367.

[11] J. W. Elam and D. H. Levy, *J. Chem. Phys.*, 1997, **106**, 10368-10378.

[12] S. L. Bernasek, M. Zappone and P. Jiang, *Surf. Sci.*, 1992, **272**, 53-64.

[13] D. A. Mantell, K. Kunimori, S. B. Ryali, G. L. Haller and J. B. Fenn, *Surf. Sci.*, 1986, **172**, 281-302.

[14] G. W. Coulston and G. L. Haller, *J. Chem. Phys.*, 1991, **95**, 6932-6944.

[15] C. Wei and G. L. Haller, *J. Chem. Phys.*, 1995, **103**, 6806-6810.

[16] D. J. Bald, R. Kunkel and S. L. Bernasek, *J. Chem. Phys.*, 1996, **104**, 7719-7728.

[17] H. Uetsuka, K. Watanabe, H. Ohnuma and K. Kunimori, *Chem. Lett.*, 1996, **25**, 227-228.

[18] T. Yamanaka and T. Matsushima, *Rev. Sci. Instrum.*, 2007, **78**, 034105.

[19] A. Alavi, P. Hu, T. Deutsch, P. L. Silvestrelli and J. Hutter, *Phys. Rev. Lett.*, 1998, **80**, 3650-3653.

[20] C. J. Zhang and P. Hu, *J. Am. Chem. Soc.*, 2001, **123**, 1166-1172.

[21] P. Salo, K. Honkala, M. Alatalo and K. Laasonen, *Surf. Sci.*, 2002, **516**, 247-253.

[22] V. P. Zhdanov, *Surf. Sci. Rep.*, 2002, **45**, 233-326.

[23] T. Yamanaka and T Matsushima, *Phys. Rev. Lett.*, 2008, **100**, 026104.

[24] B. B. Dayton, National Symposium on Vacuum. Technology Transactions (Pergamon, London1957) p. 5.

[25] K. Nakao, S. Ito, K. Tomishige and K. Kunimori, *J. Phys. Chem.,* B 2005, **109**, 17553-17559.

[26] K. Nakao, S. Ito, K. Tomishige and K. Kunimori, *J. Phys. Chem.,* B 2005, **109**, 17579-17586.

[27] K. Nakao, S. Ito, K. Tomishige and K. Kunimori, *J. Phys. Chem.,* B 2005, **109**, 24002-24007.

[28] V.R. Dhanak, G. Comelli, G. Paolucci, KC. Prince and R. Rosei, *Surf. Sci.*, 1992, **260**, L24-L27.

[29] H. Tanaka, J. Yoshinobu and M. Kawai, *Surf. Sci.*, 1995, **327**, L505-509.

[30] T. Matsushima, K. Shobatake, Y. Ohno and K. Tabayashi, *J. Chem. Phys.*, 1992, **97**, 2783-2789.

[31] W. W. Crew and R. J. Madix, *Surf. Sci.*, 1996, **349**, 275-293.

[32] T. M. Pedersen, W. X. Li and B. Hammer, *Phys. Chem. Chem. Phys.*, 2006, **8**, 1566-1574.

Figure Captions

Fig. 1 Method for determination of T_a. (a) Chemiluminescence intensities are normalized by CO_2 mass signals. Then normalized intensities of chemiluminescence from product CO_2 and reference high-temperature CO_2 from a molecular beam source are compared. (b) Details of structure and setup of the CO2 beam source. (c) Thin lines and thick curves show the chemiluminescence spectrum from reference CO_2 and optimum simulated results, respectively. (d) Determination of T_a by plotting chemiluminescence intensity normalized by CO_2 mass signals. The curve indicates theoretical calculation (see text).

Fig. 2 Curve fitting to determine T_{sb} and T_{rot}. Assuming T_a values obtained by the method shown in Fig. 1, chemiluminescence spectra from product CO_2 (thin lines) are fitted by simulated curves. The thick curves are the optimum simulated curves. The dashed curve in (b) is the optimum simulated curve obtained for the spectrum in (a). The ratio of exposure of O_2 to that of CO was 1/2 (O_2/CO=1/2) and the total exposure was 4.5×10^{17} molecules/cm^{2}s. The values of T_a, T_{sb}, and T_{rot} were 1400 K, 1530 K and 950 K (0˚), and 1050 K, 1250 K and 550 K (40˚ in [001]), respectively.

Fig. 3 Rate of CO_2 formation on Pd(110) as a function of sample temperature, T_{sample}. Rate of total exposure of CO and O_2 was 4.5×10^{17} molecules/cm^{2}s. The ratio of exposure, O_2/CO, was changed.

Fig. 4 Angular dependence of T_a (squares), T_{sb} (triangles) and T_{rot} (circles). Opened and closed symbols are results in [1$\bar{1}$0] and [001] directions, respectively. (a), (b) and (c) show results at O_2/CO = 2, 1/2 and 1/8, respectively.

Fig. 5 Models of TS structures. (a) Pd(110)(1×1) (O_2/CO = 1/2 and 1/8). (b) Pd(110) with missing-rows (O_2/CO = 2). (c)-(e) Detailed pictures of TS and desorption dynamics on Pd(110) with missing-rows (O_2/CO = 2).

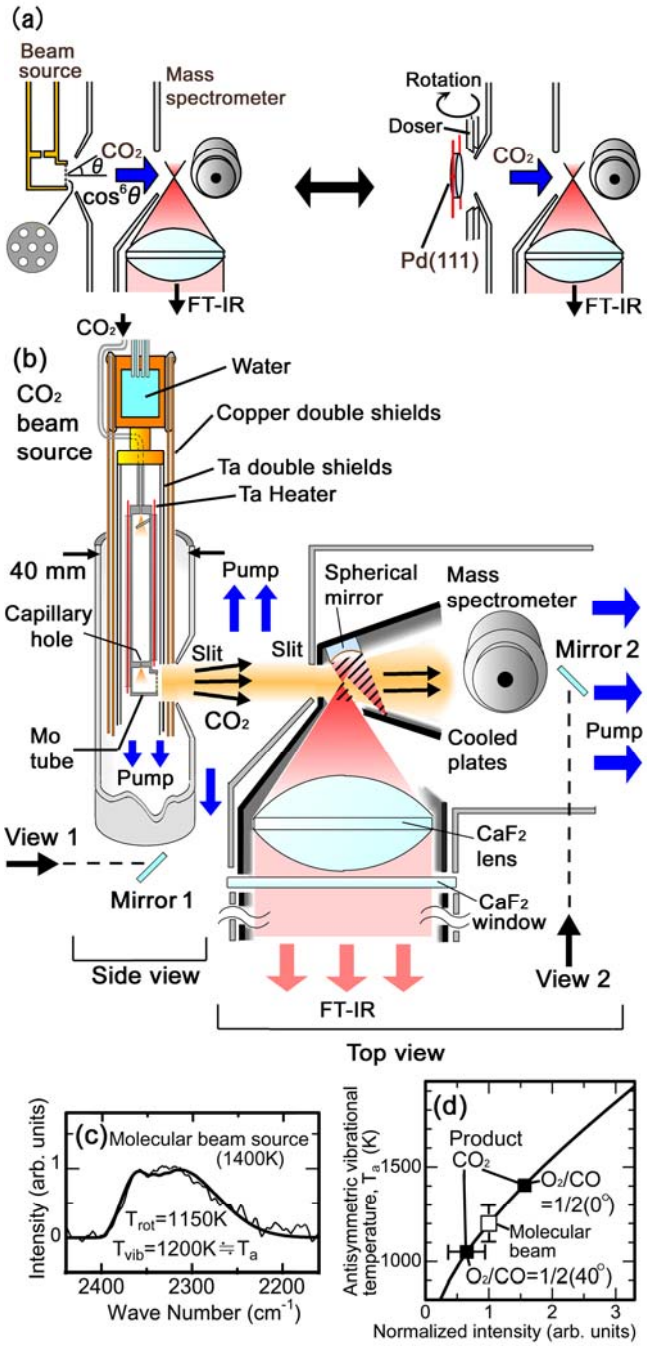
(a)
Beam source
Mass spectrometer
CO2
θ
cos6θ
FT-IR
Rotation
Doser
Pd(111)
(b)
CO2 beam source
Water
Copper double shields
Ta double shields
Ta Heater
40 mm
Pump
Capillary hole
Slit
Spherical mirror
Mass spectrometer
Mirror 2
Mo tube
Cooled plates
View 1
Mirror 1
CaF2 lens
CaF2 window
Side view
View 2
Top view
(c) Molecular beam source (1400K)
Trot=1150K
Tvib=1200K≒Ta
Intensity (arb. units)
Wave Number (cm-1)
(d)
Product CO2
O2/CO =1/2(0°)
Molecular beam
O2/CO=1/2(40°)
Antisymmetric vibrational temperature, Ta
Normalized intensity (arb. units)

Fig. 1

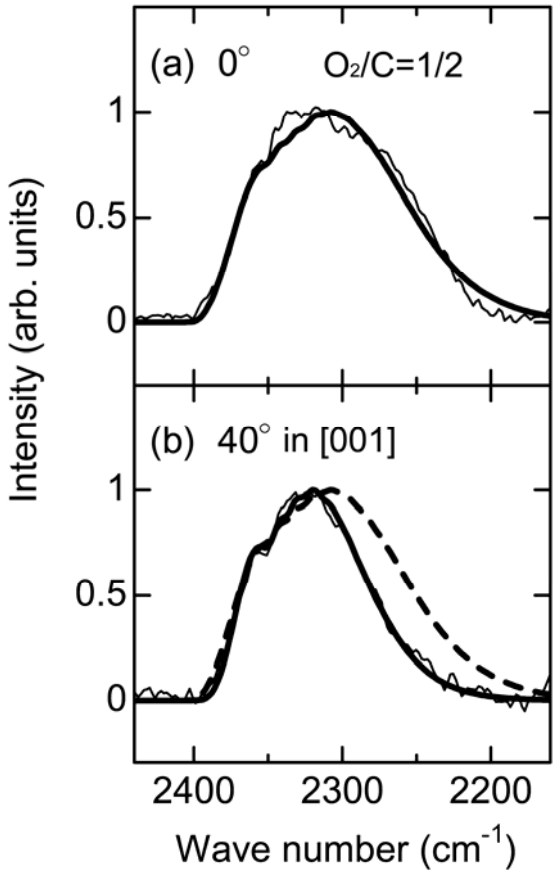
(a) 0°
O2/C=1/2
1
0.5
0
(b) 40° in [001]
1
0.5
0
Intensity (arb. units)
2400
2300
2200
Wave number (cm-1)

Fig. 2

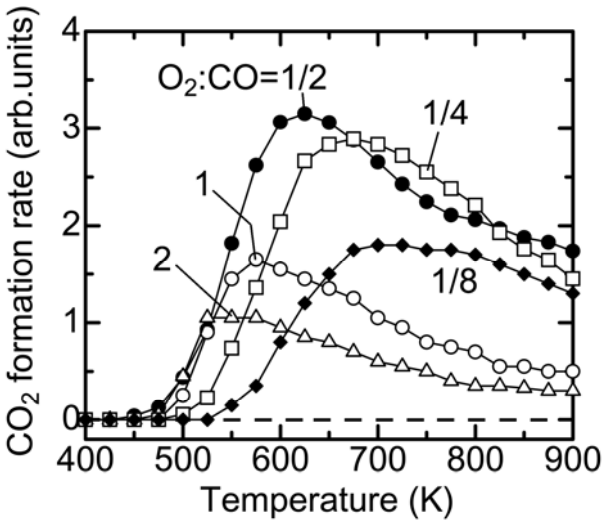
O_2:CO=1/2
1/4
1
2
1/8
CO_2 formation rate (arb.units)
Temperature (K)
0
1
2
3
4
400
500
600
700
800
900

Fig. 3

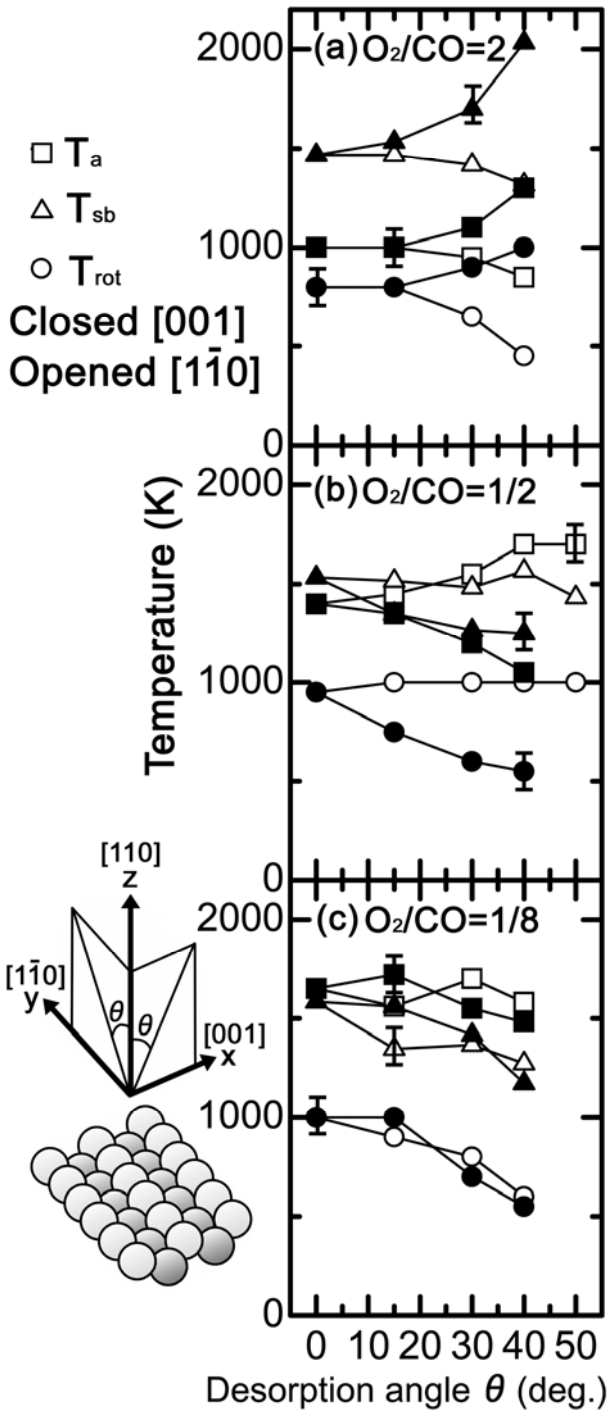
(a) O2/CO=2
(b) O2/CO=1/2
(c) O2/CO=1/8
Ta
Tsb
Trot
Closed [001]
Opened [1$\bar{1}$0]
Temperature (K)
2000
1000
0
[110]
z
[1$\bar{1}$0]
y
[001]
x
θ
θ
0 10 20 30 40 50
Desorption angle θ (deg.)

Fig. 4

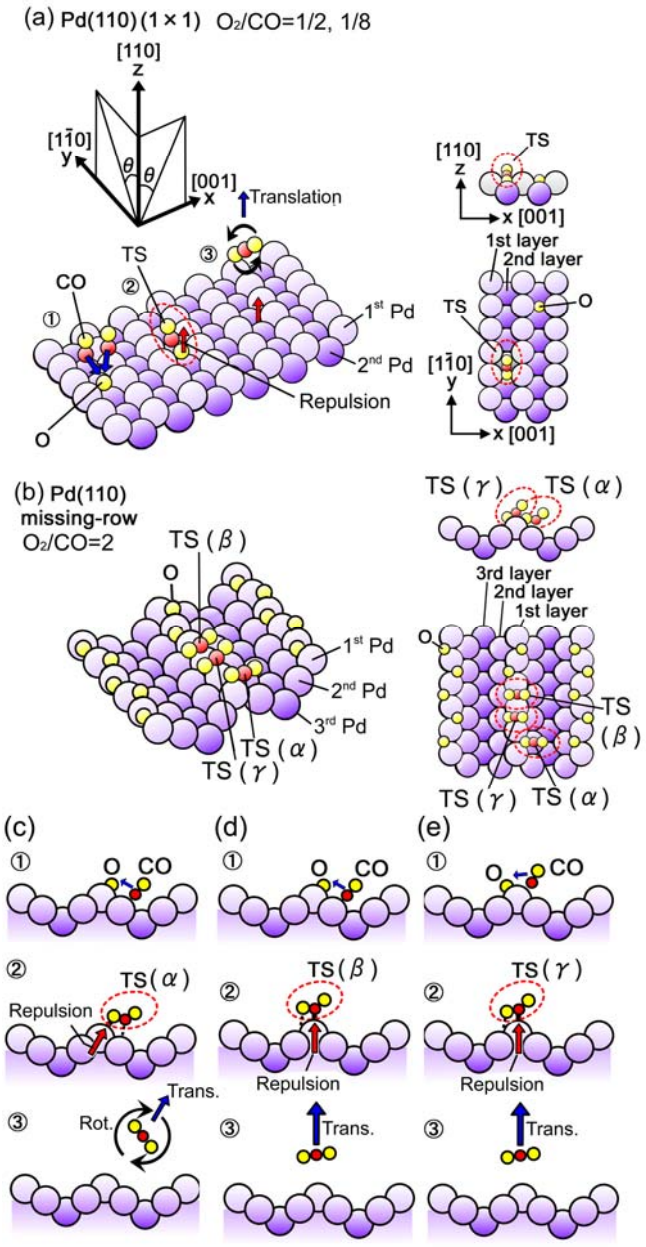
(a) Pd(110) (1 × 1) O2/CO=1/2, 1/8
[110]
z
[1$\bar{1}$0]
y
θ
θ
[001]
x
Translation
TS
③
②
CO
①
1st Pd
2nd Pd
Repulsion
O
[110]
z
TS
x [001]
1st layer
2nd layer
TS
O
[1$\bar{1}$0]
y
x [001]
(b) Pd(110)
missing-row
O2/CO=2
TS (β)
O
1st Pd
2nd Pd
3rd Pd
TS (α)
TS (γ)
TS (γ)
TS (α)
3rd layer
2nd layer
1st layer
O
TS
(β)
TS (γ)
TS (α)
(c)
(d)
(e)
①
O
CO
②
TS(α)
Repulsion
③
Rot.
Trans.
TS(β)
Repulsion
Trans.
TS(γ)
Repulsion
Trans.

Fig. 5

Graphical contents entry

Rotational and vibrational energies of product CO_2 in CO oxidation on Pd(110) surfaces were measured as functions of desorption angles. The antisymmetric vibrational temperature (T_a) was separately determined from the other vibrational modes from the normalized chemiluminescence intensity. The rotational temperature (T_{rot}) and vibrational temperature averaged over the symmetric and bending modes (T_{sb}) were then determined by the position and width of spectra by comparison with simulated spectra. On Pd(110)-(1×1), with increases in desorption angle, T_a, T_{sb} and T_{rot} decreased in the [001] direction but remained constant in [1$\bar{1}$0]. However, such anisotropy disappeared when the ratio of exposure of O_2 to that of CO decreased, resulting in a gradual decrease of the three temperatures with increases in the desorption angle. On Pd(110) with missing-rows, the three temperatures increased in [001] but decreased in [1$\bar{1}$0], indicating that the transition state changes with the geometry of the substrate. On Pd(110) with missing-rows, T_a was significantly lower than T_{sb}, although T_a was close to or higher than T_{sb} on Pd(110)-(1×1). However, there was no significant difference in angular dependence between T_a, T_{sb} and T_{rot}.